Tropical and Extratropiocal Teleconnections Associated with the Indian Summer Monsoon and the ENSO

Tetsuzo Yasunari

Institute of Geosicence, University of Tsukuba

Ibaraki 305, Japan

1. Introduction

In our previous studies(Yasunari, 1987 a, b), we showed that the ENSO involves the global circulation changes through the evolution of the entire cycle. In the tropics, the eastward propagation of wind field anomalies from the Indian Ocean toward the eastern Pacific is noticeable. In the northern mid and high latitudes, the sea-saw of circulation anomalies between the north Pacific and Eurasia is found at the intermediate stage from the anti-El Nino to El Nino (and vice versa). The circulation anomalies over Eurasia is coupled with that over India/Indian Ocean, which in turn initiates the eastward propagation of the anomalies along the tropics (Barnett, 1985; Yasunari, 1985). That is, the atmospheric process over Eurasia through the Indian Ocean seems to have key role on the mechanism of the ENSO cycle. The current study attempt to solve this problem, particularly on the role of the Indian summer monsoon on the interactions between the northern high latitudes and the tropics with the interannual time scales.

2. Seasonally-stratified ENSO anomalies

Figure 1 shows the latitude-time section of composite anomalies of velocity potential at 700mb along the tropics (20N - 10S) stratified seasonally from the fall (September to November) of a year before the El Nino years (1965, 69,72,76) to the summer (June to August) of a year after the El Nino years. The center of divergent wind anomalies (weaker convection) first appear over the Indian Ocean in spring of the El Nino Year (ENSO), and shift eastward to the western/central Pacific in summer through winter of this year.

The distribution of velocity potential anomalies in fall (October to November) of EN(0) (Fig. 2) evidently shows the reduced convection in the ITCZ over the western Pacific and in the SPCZ in the southern Pacific. Thus, the eastward propagation of divergent wind field anomalies along the tropics actually appear in the seasonal migration of reduced (or enhanced)

convection center from the Indian summer monsoon region toward the Indonesian winter monsoon region. That is to say, the ENSO-related anomalies seems to be transmitted all the time one way from the India/Indian Ocean region to the Indonesia/western Pacific region in the seasonal migration of circulation system from northern summer to northern winter. Actually, the correlation between the Indian summer monsoon rainfall (January to September) and the succeeding Indonesian winter monsoon rainfall (December to February) is relatively high (r=0.59), while the correlation between the summer monsoon rainfall and the preceding winter monsoon rainfall is very low (r=0.18). This east-ward propagation of atmospheric anomalies with interannual time scales from the Indian Ocean toward the Pacific basin has been recently scrutinized by Meehl (1987).

Figure 3 shows the latitude-time section of composite streamfunction anomalies along mid-latitudes (40N-60N) produced in the same manner as Fig. 1. The negative anomalies over central Asia appear coupled with positive anomalies over north Pacific in winter of EN(-1). Through the seasonal march from winter of EN(-1) to the fall of EN(0), the negative anomalies spread over the eastern hemisphere. In winter of EN(0) through spring of EN(1), the overall pattern is reversed in sign to the previous winter, with positive anomalies over central Asia and negative anomalies over north Pacific. Thus, the circulation changes associated with ENSO cycle can be clearly shown in the seasonally-stratified anomalies.

3. Indian summer monsoon and ENSO

High positive correlation between the Indian monsoon rainfall and the Southern Oscillation Index (SOI) has been well recognized (Pant and Parthasarathy, 1981; Rassmusson and Carpenter, 1983, etc.). Though Indian monsoon rainfall show strong biennial or triannual oscillation (Bhalme and Mooley, 1980) while SOI has a little bit larger time scale (3 - 6 years), these two phenomena still seem to be highly associated with each other. Figure 4 shows the dominant mode of global circulation anomalies at 200mb, which occupies 38.3% of the total interannual variances. The spatial pattern (Fig. 4 (a)) shows the anomalous circulation associated with typical El Nino/ anti-El Nino overturnings (Yasunari, 1987 b). However, the time coefficients (Fig. 4(b)) suggest that this mode also corresponds to anomalous circulation in the year of active/ weak Indian summer monsoon, though the extreme values correspond with the El Nino/ anti-El Nino. In other words, ENSO may be considered as the extremely amplified mode of tropical anomalous circulation which is fundamentally modulated by the Indian summer monsoon.

4. Evolution of teleconnection patterns associated with Indian summer monsoon

As has been described already, the weaker Indian summer monsoon is a necessary or otherwise a very favorable condition

for the initiation of El Nino over the Pacific, which is further preceded by the cyclonic circulation anomalies over central Asia in winter of EN (-1)(Fig. 3). This cyclonic anomalies may be closely associated with the more extensive snow cover over Eurasia (Hahn and Shukla, 1976, etc.).

To examine how the Indian summer monsoon modulates or is modulated by the high-latitude circulation with interseasonal and year-to-year time range, lag-correlation were computed between the Indian summer monsoon rainfall and dominant modes of teleconnection pattern at 500mb.

The dominant modes of teleconnection patterns were deduced from varimax-rotated principal components based on smoothed monthly 500mb geopotential height anomalies (Fig. 5). The dominant teleconnection patterns thus objectively deduced are surprinsingly correspond well with those subjectively deduced by Wallace and Gutzler (1981).

Figure 6 shows the lag-correlations between the monsoon rainfall and the time coefficients of each mode. It is noteworthy that EU pattern with negative anomalies over central Asia (comp. 4) apparently exist in fall to early winter of Y(-1) as a preceding signals of weaker summer monsoon. At nearly the same time (winter of Y(-1)) the reversed PNA pattern (comp. 2) appears with positive anomalies over the north Pacific. This combination of EU and reversed PNA pattern evidences the sea-saw of circulation anomalies as shown in Fig. 3. Interestingly, the EU pattern is rapidly reversed in sign in late winter of Y(0), which may be presumably associated with the effect of extended snow cover over central Asia. This large-scale snow cover-atmospheric interaction over Eurasia has been discussed very recently by Morinaga and Yasunari (1987).

The PNA pattern with negative anomalies over the north Pacific is likely to appear during late summer of Y(0), corresponding to weaker north Pacific high (not stronger Aleutian low) associated with weaker monsoon activity over Asia and western Pacific.

In the succeeding fall and winter of weak summer monsoon, WP pattern with negative anomalies to the north of Japan (reversed pattern of comp. 5) easily appears, which represents the weaker winter monsoon in the far-east region. This WP pattern may be associated with the weaker (or stronger) local Hadley circulation coupled with the weaker (or stronger) convection in winter over the western Pacific. Thus, the weaker (stronger) summer monsoon over south Asia is very likely to be followed by the weaker (stronger) winter over east Asia and Indonesia. This summer-to-winter coupling is significantly shown in the seasonal tendency of surface temperature anomalies in Japan (Yasunari and Yamane, 1987).

It should be noted that the PNA pattern, which frequently appear during autumn/winter of El Nino year, is not necessarily a dominant feature in the autumn/winter of Y(0). This may imply that the east-west oriented dipole pattern of convection anomalies over the equatorial Pacific (Lau and Boyle, 1987) may be efficient for producing the typical PNA pattern.

Another distinct feature in Fig. 6 is the feasible occurrence of Arctic/North Asia pattern with negative anomalies

over north Siberia through the Arctic region in the early summer of the preceding year (Y(-1)). This seems to suggest the hypothetic process that the cold air accumulated over the Siberia/arctic region during relatively stronger monsoon season (the reversed comp. 2) is apt to move down toward central Asia during the following fall and winter, producing the EU pattern (comp. 4), which in turn may lead the weaker summer monsoon in the following year as discussed already.

5. Conclusions

The change of global anomalous circulation through the ENSO cycle described in the previous studies (Yasunari, 1987 a, b) have also proved to be reconstructed with seasonally-stratified composite anomalies. This change of anomalous circulation fundamentally shows a common feature for those associated with the interannual variation of Indian summer monsoon with QBO or triannual mode. The El Nino event in the Pacific seems to be a part of response to the preceding weaker summer monsoon.

The lag-correlations shows that significant changes of dominant teleconnection patterns through season to season in the northern mid-latitudes are closely connected with the stronger (weaker) summer monsoon of each year. Particularly, the intensity of EU pattern in fall through early winter have proven to be a significant preceding signal to the following summer monsoon. Thus, the potential predictability of ENSO may exist in the predictability of Indian summer monsoon. The question is, however, still open of which case the extreme events in the equatorial Pacific may be raised or not. The process in the Southern hemisphere (Krishnamurti et al., 1986) should also be examined to solve this question.

Acknowledgements

The author wishes to thank Ryuichi Kawamura, Akihiko Murata, and Shao-fen Tian for computing assistance. Thanks are extended to Yuki Morinaga and Hye-Sook Park for editing the manuscript and drafting the figures.

References

Barnett, T.P., 1985: Variations in near-global sea level pressure. J.Atmos.Sci.,42,478-501.

Bhalme, H.N. and D.A. Mooley, 1980: Large-Scale Droughts/Floods and Monsoon Circulation. Mon.Wea.Rev., 108,1197-1211

Hahn, D.J. and Shukla, 1976: An apparent relationship between Eurasian snow cover and Indian summer monsoon rainfall. J.Atmos.Sci.,33,2461-2462.

Krishnamurti, T.N., S.H. Chu and W. Iglesias, 1986: On the sea level pressure of the Southern Oscillation.

Arch.Met.Geoph.Biol.,Ser.A,385-425.
Lau, K.M. and J.S. Boyle, 1987: Tropical and Extratropical Forcing of the Large-scale Circulation: A Diagnostic Study. Mon.Wea.Rev.,115,2,400-428.
Meehl, G.A., 1987: The Annual Cycle and Interannual Variability in the Tropical Pacific and Indian Ocean Regions. Mon.Wea.Rev.,115,1,27-50.
Morinaga, Y. and T. Yasunari, 1987: Interactions between the Snow Cover and the Atmospheric Circulations in the Northern Hemisphere. (Proc. Vancouver Symp., 1987) IAHS Publ. (In print).
Pant, G.B. and B.Parthasarathy, 1981: Some aspects of an association between the Southern Oscillation and Indian summer monsoon. Arch.Met.Geoph.Biokl.,Ser.B,29,245-252.
Rassmusson, E.M. and T.H. Carpenter, 1983: The relationship between eastern equatorial Pacific sea surface temperature and rainfall over India and Sri Lanka. Mon.Wea.Rev.,111,517-528.
Wallace, J.M. and D.S. Gutzler, 1981: Teleconnections in the Geopotential Height Field during the Northern Hemisphere Winter. Mon.Wea.Rev.,109,784-812.
Yasunari, T., 1985: Zonally propagating modes of the global east-west circulation associated with the Southern Oscillation. J.Met.Soc.Japan,63,1013-1029.
_____, 1987 a: Global Structure of the El Nino/Southern Oscillation Part I. El Nino Composites. J. Met.Soc.Japan,65,67-80.
_____, 1987 b: Global Structure of the El Nino/Southern Oscillation Part II. Time Evolution. J.Met.Soc.Japan,65,81-102.
_____ and Yamane, 1987: Climatic change deduced from the anomalous seasonal cycle. (To be published)

Fig. 1. Latitude-time section of composite velocity potential anomalies at 700 mb along 20N-10S. EN(-1) denotes the year before the El Nino year, E(0) denotes the El Nino year and E(+1) denotes the year after the El Nino year, respectively. Positive values (solid lines) show divergent wind anomalies.

Fig. 2. Composite anomalies of velocity potential at 700 mb for the fall (SON) of El Nino year (1965,69,72,76). Positive values (solid lines) denote divergent winds.

Fig. 3. Same as Fig. 1 but for streamfunction at 200 mb along 40N-60N. Positive values (solid lines) denote anticyclonic circulation.

Fig. 4. First eigenvectors for streamfunction anomalies at 200 mb (38.3 % of total variance) (a) and its time coefficients (b). In (b) EN denotes El Nino year, and W denotes weak summer monsoon year.

Fig. 5. Principal modes of varimax-rotated eigenvectors for smoothed monthly 500 mb geopotential height anomalies.

Fig. 6. Lag correlations between the Indian summer monsoon rainfall and time coefficients of the princial modes shown in Fig. 5. Correlations with the values of less than 0.2 are not shown. Y(-1) denotes the year before the reference monsoon year, Y(0) denotes the reference monsoon year and Y(+1) denotes the year after the reference monsoon year, respectively.

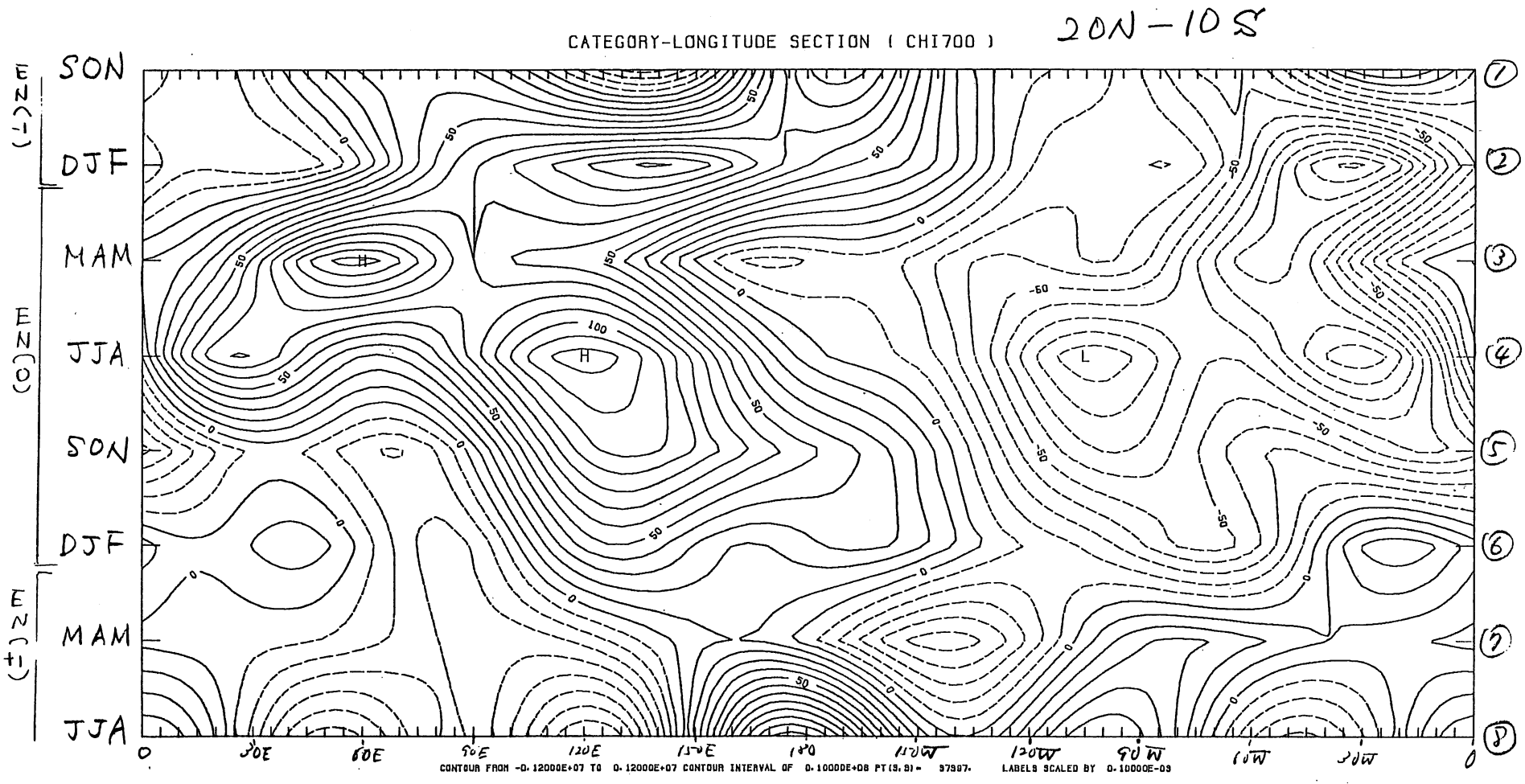

Fig. 1. Latitude-time section of composite velocity potential anomalies at 700 mb along 20N-10S. EN(-1) denotes the year before the El Nino year, E(0) denotes the El Nino year and E(+1) denotes the year after the El Nino year, respectively. Positive values (solid lines) show divergent wind anomalies.

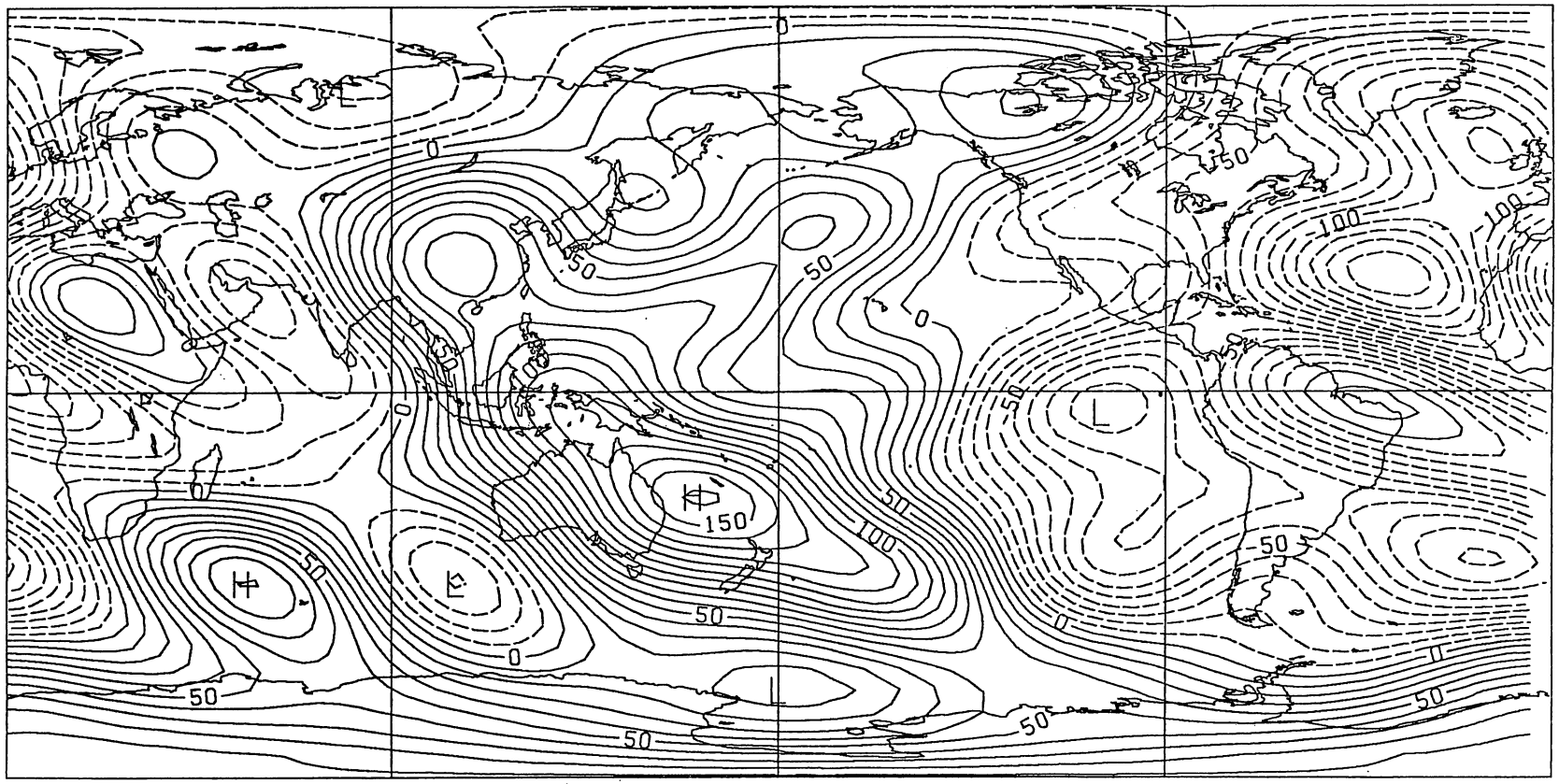

Fig. 2. Composite anomalies of velocity potential at 700 mb for the fall (SON) of El Nino year (1965,69,72,76). Positive values (solid lines) denote divergent winds.

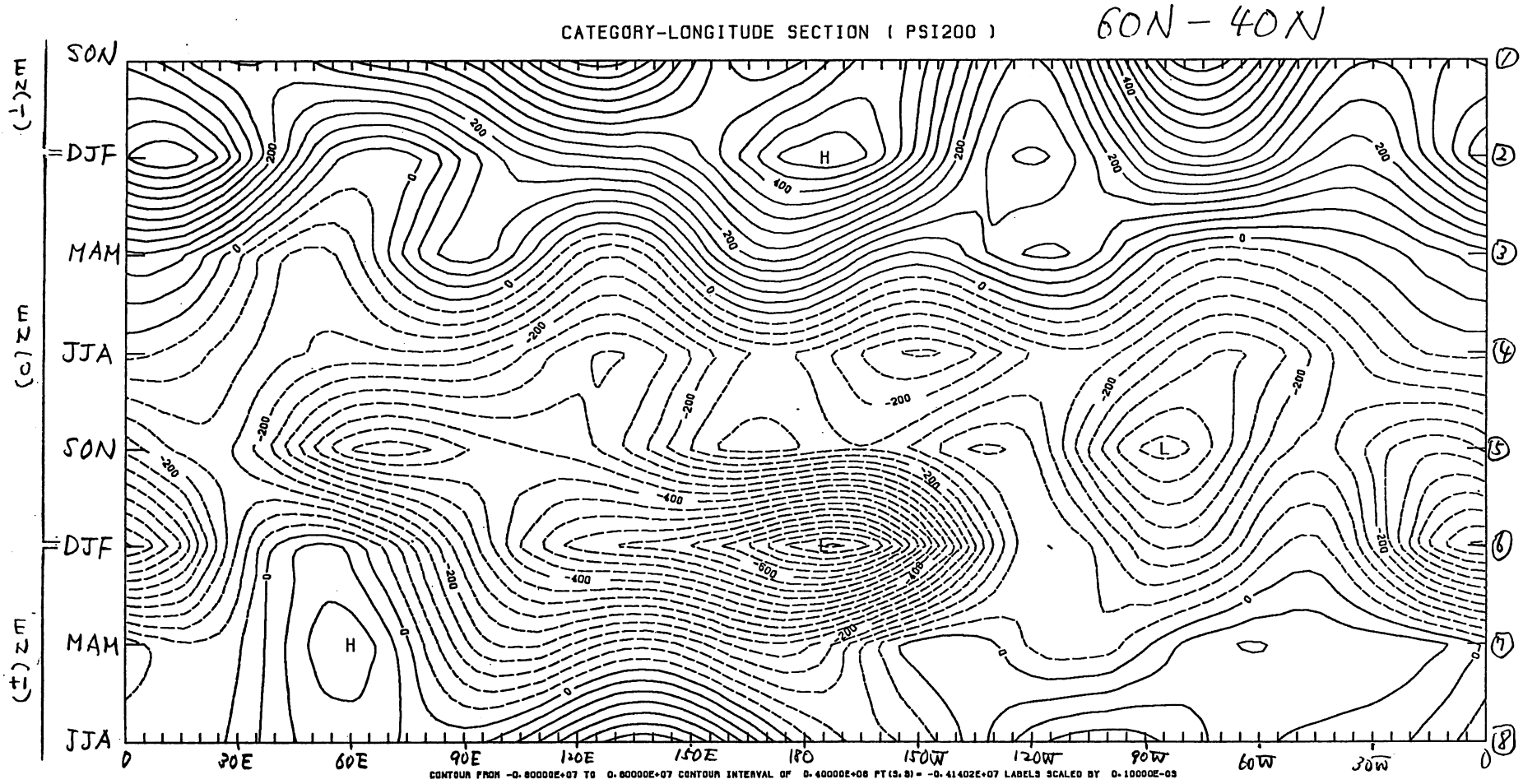

Fig. 3. Same as Fig. 1 but for streamfunction at 200 mb along 40N-60N. Positive values (solid lines) denote anticyclonic circulation.

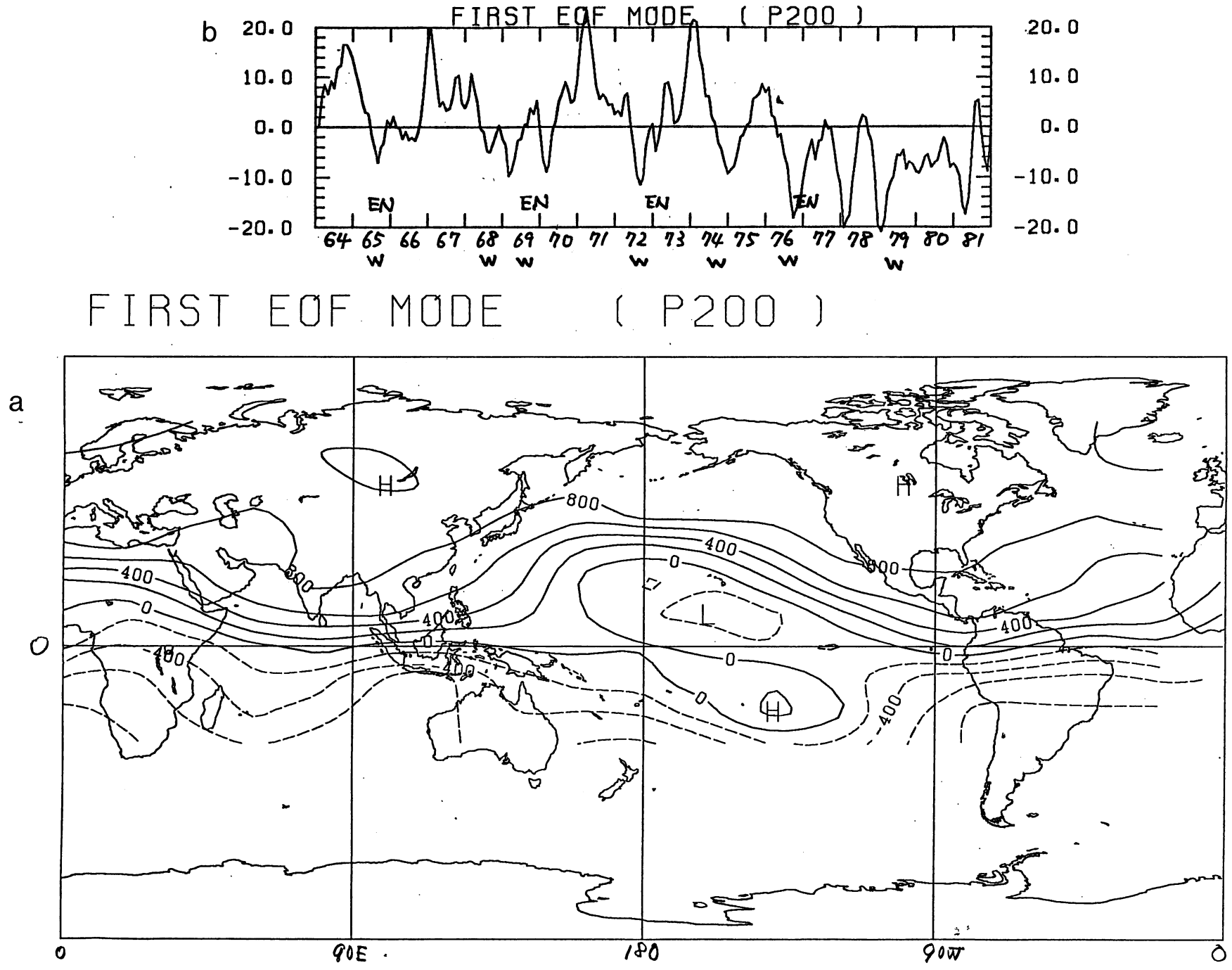

Fig. 4. First eigenvectors for streamfunction anomalies at 200 mb (38.3 % of total variance) (a) and its time coefficients (b). In (b) EN denotes El Nino year, and W denotes weak summer monsoon year.

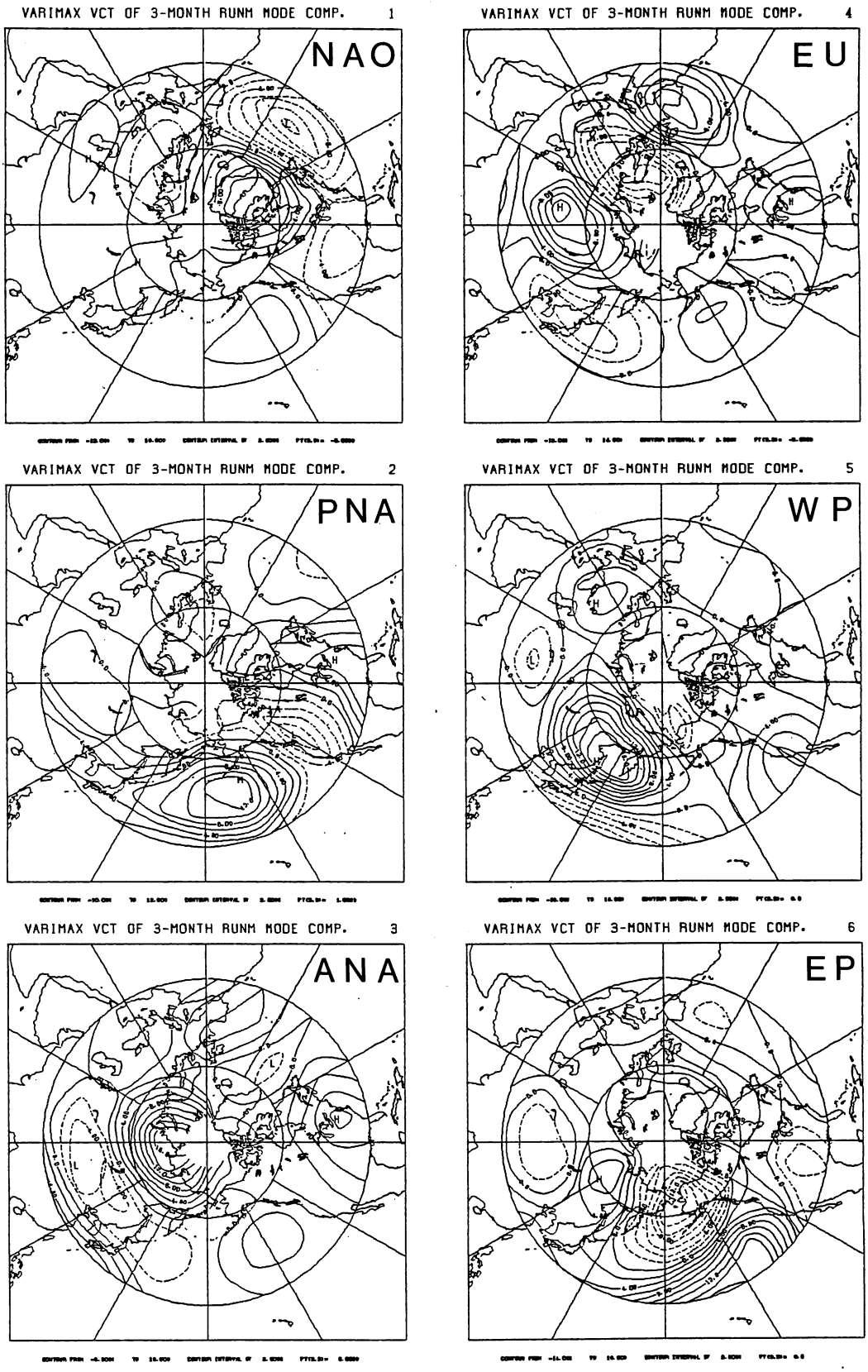

Fig. 5. Principal modes of varimax-rotated eigenvectors for smoothed monthly 500 mb geopotential height anomalies.

VARIMAX VCT OF 3-MONTH RUNM MODE COMP. 7

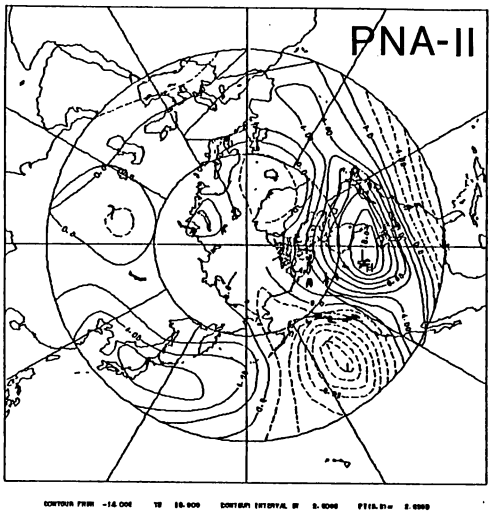

VARIMAX VCT OF 3-MONTH RUNM MODE COMP. 8

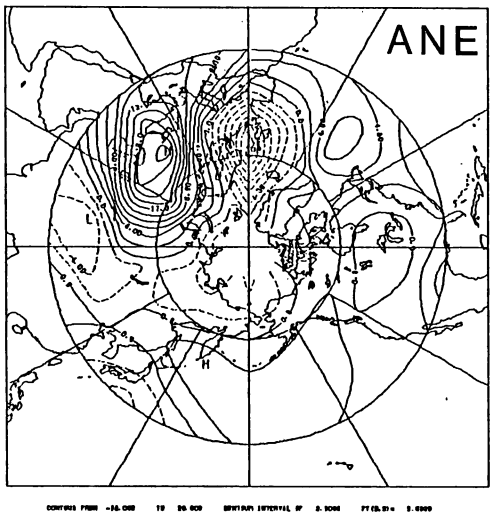

VARIMAX VCT OF 3-MONTH RUNM MODE COMP. 9

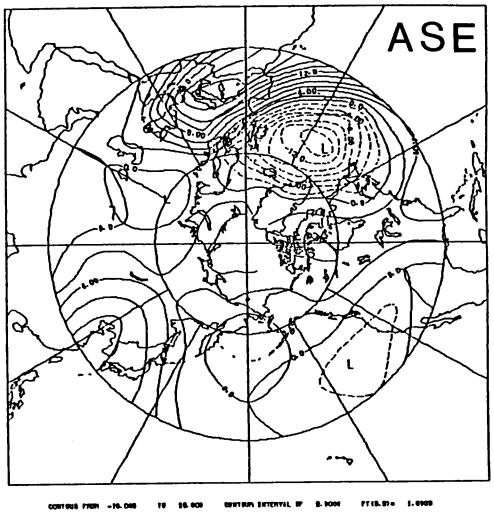

VARIMAX VCT OF 3-MONTH RUNM MODE COMP. 10

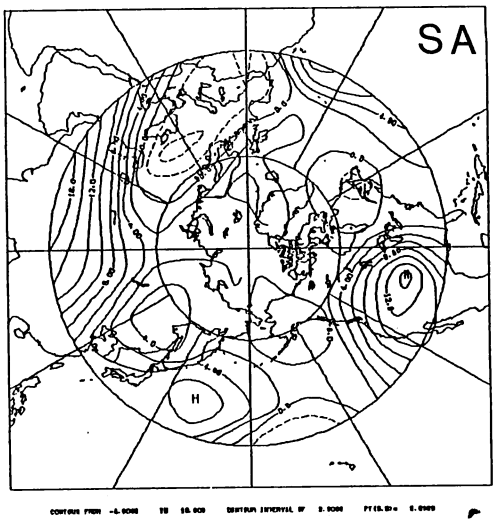

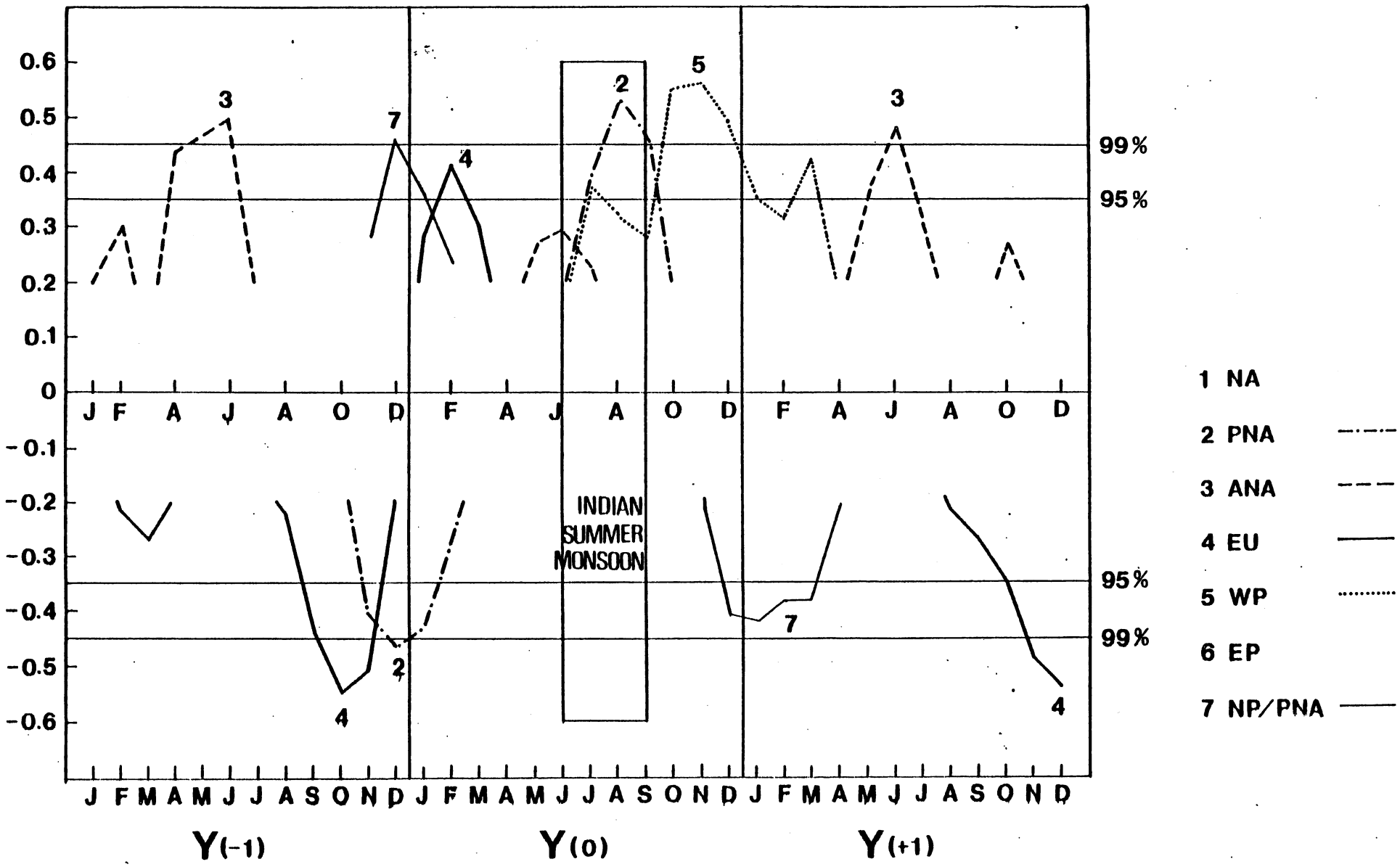

Fig. 6. Lag correlations between the Indian summer monsoon rainfall and time coefficients of the princial modes shown in Fig. 5. Correlations with the values of less than 0.2 are not shown. Y(-1) denotes the year before the reference monsoon year, Y(0) denotes the reference monsoon year and Y(+1) denotes the year after the reference monsoon year, respectively.